Functional Regulation of the Opposing (p)ppGpp Synthetase/Hydrolase Activities of Rel_{Mtb} from *Mycobacterium tuberculosis*†

Andrew Avarbock, David Avarbock, Jiah-Shin Teh, Michael Buckstein, Zhi-mei Wang, and Harvey Rubin*

Division of Infectious Diseases, Department of Medicine, University of Pennsylvania, School of Medicine, Philadelphia, Pennsylvania 19104

Received March 23, 2005; Revised Manuscript Received May 18, 2005

ABSTRACT: The dual-function Rel_{Mtb} protein from *Mycobacterium tuberculosis* catalyzes both the synthesis and hydrolysis of (p)ppGpp, the effector of the stringent response. In our previous work [Avarbock, D., Avarbock, A., and Rubin, H. (2000) *Biochemistry 39*, 11640], we presented evidence that the Rel_{Mtb} protein might catalyze its two opposing reactions at distinct active sites. In the study presented here, we purified and characterized fragments of the 738-amino acid Rel_{Mtb} protein and confirmed the hypothesis that amino acid fragment 1−394 contains both synthesis and hydrolysis activities, amino acid fragment 87−394 contains only (p)ppGpp synthesis activity, and amino acid fragment 1−181 contains only (p)-ppGpp hydrolysis activity. Mutation of specific residues within fragment 1−394 results in the loss of synthetic activity and retention of hydrolysis (G241E and H344Y) or loss of hydrolytic activity with retention of synthesis (H80A and D81A). The C-terminally cleaved Rel_{Mtb} fragment proteins have basal activities similar to that of full-length Rel_{Mtb}, but are no longer regulated by the previously described Rel_{Mtb} activating complex (RAC). Residues within the C-terminus of Rel_{Mtb} (D632A and C633A) are shown to have a role in interaction with the RAC. Additionally, size exclusion chromatography indicates Rel_{Mtb} forms trimers and removal of the C-terminus results in monomers. The C-terminal deletion, 1−394, which exists as a mixture of monomers and trimers, will dissociate from the trimer state upon the addition of substrate. Furthermore, the trimer state of fragment 1−394 appears to be a catalytically less efficient state than the monomer state.

Mycobacterium tuberculosis (Mtb) infects more than one-third of the world's population and kills more than 3 million people a year, making it the world's deadliest bacterial infection (*1*). Tuberculosis incidence as well as the development of multidrug-resistant tuberculosis has escalated because of the increasing prevalence of HIV infection, increasing rates of homelessness and incarceration, and the limited capacity of tuberculosis control programs to treat patients until they are cured (*2*). Although the disease can be treated with antimicrobial agents that kill a great majority of the tubercle bacilli in a lesion within 1 or 2 weeks, it is necessary to continue multidrug therapy for at least 5 months. This prolonged therapy maximizes the elimination of the few remaining bacilli, thereby preventing reactivation of the disease years later. It is presumed that these bacilli "persistors" lie dormant in an environment characterized, in part, by nutrient deprivation and oxygen limitation (*3*). It is also suggested that Mtb can persist in this environment by entering a state of dormancy via the process of rapidly reducing or completely switching off protein synthesis to achieve a shutdown of cellular metabolic activity.

An Mtb gene, rel_{Mtb}, encodes a protein of 738 amino acid residues and belongs to the *relA*/*spoT* family of genes that mediates a global regulation of protein synthesis known as the stringent response (*4*). A knockout strain of rel_{Mtb} (Δrel_{Mtb}) demonstrated that the enzyme is responsible for the intracellular regulation of (p)ppGpp,[1] the effector of the stringent response, and the consequent ability of Mtb to survive long-term starvation in culture (*5*). Rel_{Mtb} also regulates a broad transcriptional program encompassing more than 80 genes and is critical for the establishment of a persistent Mtb infection in mice (*6*).

Rel_{Mtb} is a member of the superfamily of single-gene-encoded bifunctional enzymes that catalyze opposing reactions (*7*). During amino acid starvation, the Rel_{Mtb} protein catalyzes the transfer of the 5′-β,γ-pyrophosphate group from ATP to the 3′-OH of GTP or GDP [ATP + GTP (GDP) ↔ AMP + (p)ppGpp]. As amino acid levels return to normal, the stringent response is reversed by Rel_{Mtb} catalyzing the hydrolysis of the pyrophosphate group (PP_i) from the 3′-OH of both pppGpp and ppGpp, yielding GTP or GDP [(p)-ppGpp → GTP (GDP) + PP_i] (*5*, *7*). Differential regulation of Rel_{Mtb}'s opposing activites by the aminoacylation state of a tRNA·ribosome·mRNA complex (Rel_{Mtb} activating complex or RAC) (*7*) allows Mtb to efficiently respond to environmental changes.

† This work was supported by NIH Grant AI43420 and DARPA Grant 730602-01-2-0563 to H.R. A.A., D.A., and M.B. are funded by the NIH Medical Scientist Training Program.

* To whom correspondence should be addressed: University of Pennsylvania, 522 Johnson Pavilion, Philadelphia, PA 19104. Telephone: (215) 662-6475. Fax: (215) 662-7842. E-mail: rubinh@mail.med.upenn.edu.

[1] Abbreviations: pppGpp, guanosine 5′-triphosphate, 3′-diphosphate; pppIpp, inosine 5′-triphosphate, 3′-diphosphate; PP_i, inorganic pyrophosphate; PEI, polyethylenimine.

10.1021/bi0505316 CCC: $30.25
Published on Web 06/29/2005

In our previous study (*7*), three pieces of evidence led us to believe that the two opposing catalytic activities of Rel_{Mtb} take place at distinct active sites: (i) the differential sensitivity of the two reactions to Mg^{2+}, (ii) the ability to synthesize but not hydrolyze pppIpp, and (iii) the simultaneous synthesis and hydrolysis of (p)ppGpp at the maximal basal rate of each reaction. On the basis of a previous study which showed that the (p)ppGpp synthesis and hydrolysis activities of SpoT, a Rel_{Mtb} homologue found in *Escherichia coli*, could be separated into distinct domains (*8*), we constructed Rel_{Mtb} fragments to test our hypotheses. In the study presented here, we confirm that Rel_{Mtb} contains distinct active sites by purifying functional synthesis and hydrolysis fragments. We also confirm that the C-terminus of Rel_{Mtb} is an important region for multimerization and regulation of (p)ppGpp synthesis and hydrolysis.

MATERIALS AND METHODS

DNA Manipulation and PCR Amplification. Rel_{Mtb} fragments were PCR-amplified from Rel_{Mtb} template DNA using Vent polymerase. The following primers were used: N-terminus, GATATACCATGGGCAGCAGCC; 87−394 N-terminus, GATTGATCCATATGGGTTACACCCTGGAGGCGTT; 1−394 and 87−394 C-terminus, GATCATGGATCCCTAGTCGTAGCGCAATGATTCCA; 1−203 C-terminus, GATCATGGATCCCTACTCCTCGTACTTCTTGGGAT; 1−181 C-terminus, GATCATGGATCCCTACATGCCCAGCCGATGCGCCAG; and 1−156 C-terminus, GATCATGGATCCCTACAAGAAGCGCATGGTGCGCAT. Restriction sites used for cloning are underlined. Amplification conditions were as follows: 30 cycles at 94 °C for 45 s, 55 °C for 45 s, and 72 °C for 3 min. The PCR products were digested with NdeI, NcoI, and BamH1 (New England Biolabs) and cloned into pET15b vectors.

Expression and Purification of Rel_{Mtb} Using E. coli as a Host. BL21[DE3] cells carrying pET15b plasmids with the appropriate fragment DNA were grown in LB medium to an OD of 0.6 for 37 °C growth (1−450, 1−394, 1−181, 395−738, G241E, H344Y, H80A, and D81A) and to an OD of 1.1 for 15 °C growth (1−203, 87−394, D632R, and D632A). Isopropyl 1-thiogalactopyranoside (IPTG) was added to a final concentration of 1.0 mM (37 °C growth) and 0.04 mM (15 °C growth), and the protein was expressed for 3 and 15 h, respectively. Cells were resuspended in buffer containing 50 mM NaP_i (pH 8.0), 300 mM NaCl, and 20 mM imidazole and then lysed with a French press. Cell debris was removed by one round of centrifugation. The lysate was added to Ni^{2+}−NTA agarose (Qiagen) for 1 h, and the resin was then transferred to a column and washed with 50 mL of 50 mM NaP_i (pH 8.0), 300 mM NaCl, and 20 mM imidazole. The His tag proteins were eluted with 50 mM NaP_i (pH 8.0), 300 mM NaCl, and 100 mM imidazole. Protein fractions were checked at OD_{280} using calculated extinction coefficients of 5120 M^{-1} cm^{-1} for fragment 1−156 (17.3 kDa), 5120 M^{-1} cm^{-1} for fragment 1−181 (20.1 kDa), 12 090 M^{-1} cm^{-1} for fragment 1−203 (22.7 kDa), 49 620 M^{-1} cm^{-1} for fragment 87−394 (35.1 kDa), and 53 460 M^{-1} cm^{-1} for fragment 1−394 (44.6 kDa) (Swiss-Prot Analysis), and purity was assessed by SDS−PAGE analysis.

The pET22b expression system (Novagen) was used to purify the 82 kDa recombinant Rel_{Mtb} protein as previously described (*5*). The concentration of wild-type Rel_{Mtb} was determined by OD_{280} using a calculated extinction coefficient of 77 170 M^{-1} cm^{-1} for full-length 82 kDa Rel_{Mtb}.

Expression and Purification of Rel_{Mtb} Using Mycobacterium smegmatis as a Host. Wild-type and Rel_{Mtb} genes with the desired mutation (D632A, D632R, and C633A) were PCR-amplified and cloned into an *E. coli*−*M. smegmatis* shuttle vector downstream of an acetamidase gene promoter (cloned from *M. smegmatis* genomic DNA) and upstream of a hexahistidine tag. This vector, carrying a hygromycin resistance gene, was constructed in our laboratory. *M. smegmatis* competent cells carrying the construct were used to inoculate 2 mL of 7H9 medium, and this starter culture was incubated at 37 °C with shaking for 2 days, and then used to inoculate larger volumes of 7H9 medium supplemented with OADC enrichment and 2% acetamide (Sigma). The culture was grown for 3 days, and cells were then harvested and resuspended in equilibration buffer [25 mM imidazole, 400 mM NaCl, and 50 mM NaP_i (pH 8.0)]. The same protein purification method in the previous section was then followed.

Transferase Assay. The transferase assay was carried out as previously described (*7*). Briefly, ribosome-independent transferase reaction mixtures (30 °C) contained 50 mM HEPES (pH 8.0), 100−225 mM NaCl, 1 mM DTT, indicated concentrations of ATP/GTP (Pharmacia), varying $MgCl_2$ or $MnCl_2$ concentrations, and enzyme. In addition, the Rel_{Mtb} activating complex (RAC) reaction mixtures included ribosomes (0.15−0.30 μM), tRNA (0.20−1.50 μM), and mRNA [2.00 μM poly(U)]. Reactions were monitored using either [γ-^{33}P]ATP or [γ-^{33}P]GTP (NEN) at 1 μCi/μmol. Reaction rates were calculated by taking 5 μL aliquots at multiple time points, spotting them onto PEI-cellulose TLC plates (Sigma-Aldrich), and developing the plates in 1.5 M KP_i (pH 3.4). Reaction products were visualized using a Storm Phosphorimager (Molecular Dynamics) and quantitated using ImageQuant version 1.2 (Molecular Dynamics).

Hydrolysis Assay. The hydrolysis assay was carried out as previously described (*7*). Briefly, hydrolysis reaction mixtures (30 °C) contained 50 mM HEPES (pH 8.0), 100−225 mM NaCl, 1 mM DTT, indicated concentrations of pppGpp, varying $MnCl_2$ concentrations, and enzyme. Preparative amounts of pppGpp were synthesized from fragment protein 1−394 and purified. The hydrolysis reaction product, $*PP_i$, was visualized and quantitated as described for the assay for the transferase reaction.

Gel Filtration Chromatography. A Superdex 200 HR 10/30 column was used to estimate the apparent molecular mass of Rel_{Mtb} multimers at room temperature. Protein samples were applied to the column system equilibrated in a standard elution buffer [50 mM HEPES buffer (pH 8.2), 250 mM NaCl, 0.1 mM DTT, and 5% glycerol] at a flow rate of 0.75 mL/min. Ribonuclease A, chymotrypsinogen A, ovalbumin, albumin, aldolase, catalase, ferritin, and thyroglobulin (Amersham Pharmacia Biotech) were used as protein standards for column calibration. Elution was monitored for protein at OD_{280}.

RESULTS

Dissection of the Bifunctional Protein into Separate Catalytic Domains. Our previous finding that the 738-amino

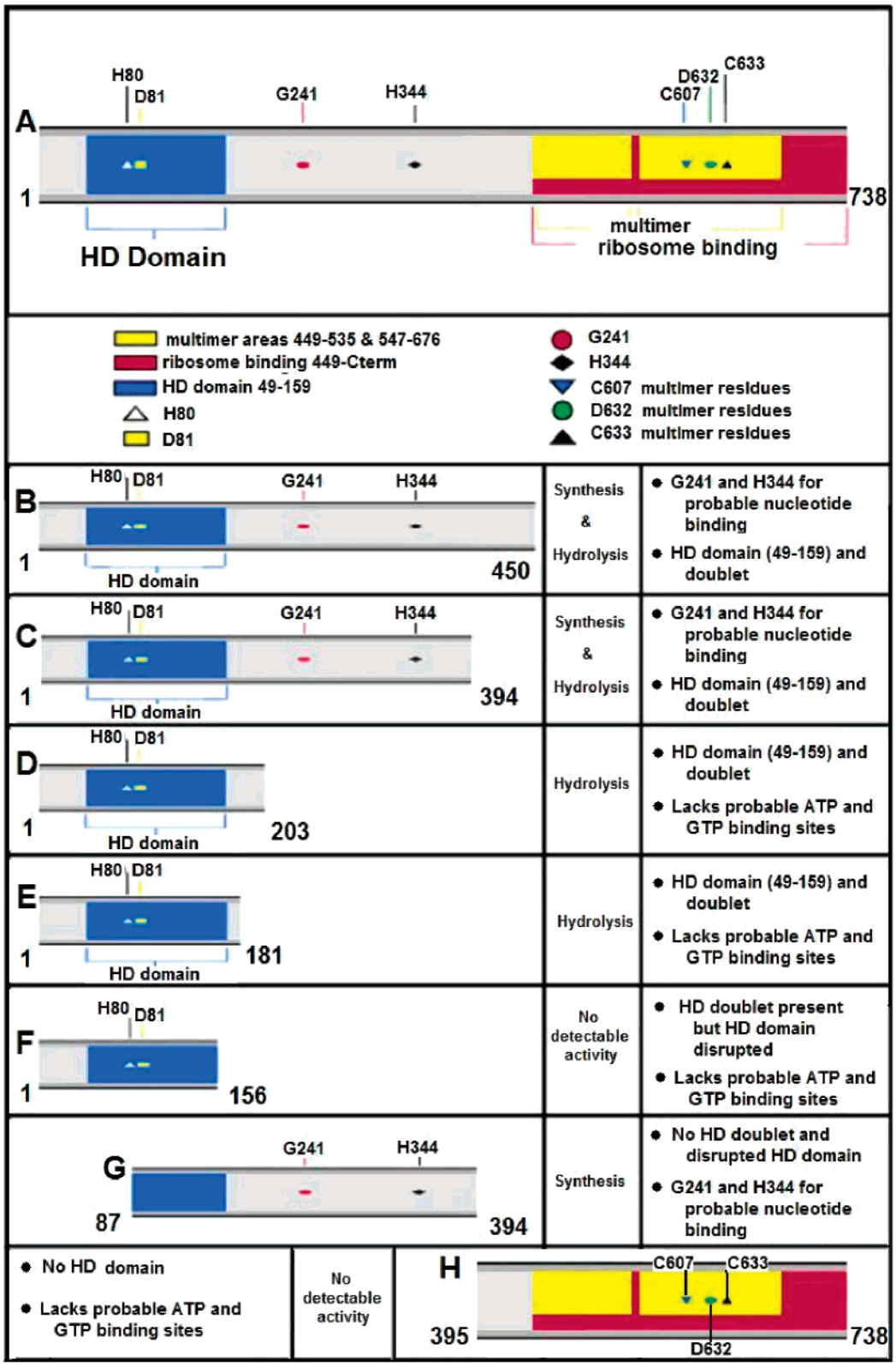

FIGURE 1: Summary of truncated Rel_{Mtb} proteins, activity, and important domains. Panel A shows full-length Rel_{Mtb}, and panels B−H show truncated proteins.

acid Rel_{Mtb} can both synthesize and hydrolyze (p)ppGpp suggested that it may have separate domains for these opposing activities. Seven fragments were expressed and purified, and three fragments with activity were characterized in detail (Figure 1): (i) amino acid fragment 1−394 capable of both pppGpp synthesis and hydrolysis, (ii) amino acid fragment 1−203 capable of only pppGpp hydrolysis, and (iii) amino acid fragment 87−394 capable of only pppGpp synthesis.

Comparison of Dual-Function Rel_{Mtb} Fragments to Wild-Type Rel_{Mtb}. To determine whether both of the catalytic activities of Rel_{Mtb} could be localized to a smaller region, three truncated proteins were expressed and purified: amino acid fragments 1−450, 1−394, and 395−738 (Figure 1).

Table 1: Kinetic Constants for the Rel_{Mtb} Transferase Reaction[a]

reaction	K_{GTP} (mM)	k_{cat} (s^{-1})	k_{cat}/K_{GTP} (mM^{-1} s^{-1})
(1) full-length Rel_{Mtb}	1.36 ± 0.12	0.4 ± 0.04	0.29
(2) full-length Rel_{Mtb} + $tRNA^{Phe}$	0.7 ± 0.04	0.4 ± 0.04	0.58
(3) full-length Rel_{Mtb} + $tRNA^{Phe}$·ribosomes·poly(U) (RAC)	0.33 ± 0.04	8.4 ± 0.3	25
(4) fragment 1−394 monomer	0.67 ± 0.05	0.66 ± 0.06	0.98
(5) fragment 1−394 + $tRNA^{Phe}$	0.67 ± 0.05	0.66 ± 0.06	0.98
(6) fragment 1−394 + $tRNA^{Phe}$·ribosomes·poly(U) (RAC)	0.67 ± 0.05	0.66 ± 0.06	0.98
(7) fragment 87−394	0.78 ± 0.08	0.47 ± 0.04	0.52
(8) fragment 87−394 + $tRNA^{Phe}$	0.78 ± 0.08	0.47 ± 0.04	0.52
(9) fragment 87−394 + $tRNA^{Phe}$·ribosomes·poly(U) (RAC)	0.78 ± 0.08	0.47 ± 0.04	0.52

[a] The transferase reaction that was assayed was *pppA (*ATP) + pppG (GTP) ↔ pA (AMP) + pppGpp*. pppGpp* indicates that the radioactive label is on the 3′-PP_i group of the ribose ring of GTP. Reactions were performed at 30 °C and pH 8.0. For the determination of K_{GTP}, the ATP concentration was held constant (15 mM, 1 μCi/μmol of [γ-^{33}P]ATP). The k_{cat} was calculated as if all components in the reaction were in a monomer state.

Table 2: Relative Activity of pppGpp Hydrolysis by Rel_{Mtb} Variants[a]

reaction	mol of PP_i s^{-1} (mol of enzyme)$^{-1}$
(1) full-length Rel_{Mtb}	0.028
(2) fragment 1−394 monomer	0.027
(3) fragment 1−203	0.03
(4) fragment 1−181	0.00021

[a] The hydrolysis reaction that was assayed was pppGpp* (pppGpp) → *PP_i + pppG (GTP). pppGpp* indicates that the radioactive label is on the 3′-PP_i group of the ribose ring of GTP. Reactions were performed for 20 min at 30 °C and pH 8.0 with 0.1 mM pppGpp. Moles of enzyme were determined as if all of the enzyme was in a monomer state.

Fragment proteins 1−450 and 1−394 were capable of synthesis and hydrolysis and had similar activities, while fragment protein 395−738 was devoid of any activity. Fragment 1−394 had a k_{cat} for pppGpp synthesis similar to that of wild-type Rel_{Mtb}, and a K_m for GTP ~2-fold lower than that of wild-type Rel_{Mtb} (Table 1, reaction 1 vs reaction 4). The relative activity of Rel_{Mtb} fragment 1−394 and wild-type Rel_{Mtb} for pppGpp hydrolysis was nearly the same (Table 2, reaction 1 vs reaction 2).

Comparison of pppGpp Hydrolysis-Only Fragments to Wild-Type Rel_{Mtb}. Three fragments were purified and assayed to determine the domain necessary for pppGpp hydrolysis: amino acid fragments 1−203, 1−181, and 1−156 (Figure 1). Amino acid fragments 1−203 and 1−181 possessed pppGpp hydrolysis activity but were incapable of pppGpp synthesis activity. Amino acid fragment 1−156 was not capable of either pppGpp synthesis or hydrolysis. The relative activity of amino acid fragment 1−203 was similar to that of wild-type Rel_{Mtb} (Table 2, reaction 1 vs reaction 3), while the relative activity of fragment 1−181 decreased approximately 130-fold compared to that of wild-type Rel_{Mtb} (Table 2, reaction 1 vs reaction 4).

Comparison of a pppGpp Synthesis-Only Fragment to Wild-Type Rel_{Mtb}. A fragment containing amino acids 87−394 was found to have only pppGpp synthesis activity. The k_{cat} for protein fragment 87−394 was similar to that of wild-type Rel_{Mtb}, while the K_m for GTP was approximately 2-fold lower (Table 1, reaction 1 vs reaction 7).

Metal Requirements for Transferase and Hydrolysis Reactions. We previously described (*7*) a very narrow divalent cation concentration range required for the maximal activity of wild-type Rel_{Mtb}: the optimal Mg^{2+} concentration for pppGpp synthesis was approximately equal to the total concentration of nucleotide substrates ([ATP] + [GTP]), whereas the optimal Mn^{2+} concentration was approximately one-half of the total concentration of nucleotide substrates. Rel_{Mtb} fragments 1−394 and 87−394 also had the same metal concentration range requirements for the transferase reaction as wild-type Rel_{Mtb}. Like in wild-type Rel_{Mtb}, only Mn^{2+} is capable of supporting the hydrolysis reaction for the truncated Rel_{Mtb} proteins.

Identification of Essential Residues for Rel_{Mtb} pppGpp Synthesis. The *E. coli* RelA G251E mutation impaired both ATP and GTP binding and caused a complete loss of RelA (p)ppGpp synthesis ability in culture, and a RelA H354Y mutation impaired ATP binding and caused a partial loss of synthetic activity (*9*). RelA G251 and H354 are conserved in wild-type Rel_{Mtb} and correspond to Rel_{Mtb} G241 and H344, respectively (Figure 1A). We mutated both of these residues in Rel_{Mtb} fragment protein 1−394, creating two separate mutants, G241E and H344Y. Both the G241E and H344Y mutants retained pppGpp hydrolytic activity, with hydrolysis kinetics similar to that of 1−394, but both lost the ability to synthesize pppGpp (Figure 2).

Identification of Essential Residues for Rel_{Mtb} (p)ppGpp Hydrolysis. Rel_{Mtb} contains a histidine and aspartate doublet (H80-D81) that has been identified as part of a conserved region known as the HD domain (Figure 1A) (*10*). The histidine and aspartate residues are predicted to be essential for coordinating divalent cations (*10*, *11*), and thus may be essential for Rel_{Mtb}. We mutated each of these residues in Rel_{Mtb} fragment protein 1−394, creating two mutants, H80A and D81A. Both the H80A and D81A mutants were capable of pppGpp synthesis, with synthesis kinetics similar to that of the 1−394 protein, but were not capable of pppGpp hydrolysis (Figure 2).

Higher-Level Regulation of Rel_{Mtb} Activity by the Rel_{Mtb} Activating Complex (RAC). In our previous study, adding only uncharged tRNA to the full-length Rel_{Mtb} ribosome-independent transferase reaction mixture caused a 2-fold decrease in K_{ATP} and K_{GTP} (Table 1, reaction 1 vs reaction 2) (*7*). Addition of a complex of uncharged tRNA, ribosomes, and cognate mRNA (RAC) to the wild-type Rel_{Mtb} transferase reaction mixture lowered K_{ATP} and K_{GTP} 4-fold and increased k_{cat} 20-fold (Table 1, reaction 1 vs reaction 3). In contrast, Rel_{Mtb} fragments 1−394 and 87−394 with (p)ppGpp transferase activity failed to be activated above basal levels by uncharged tRNA alone or the Rel_{Mtb} activating complex (RAC) (Table 1, reactions 4−9).

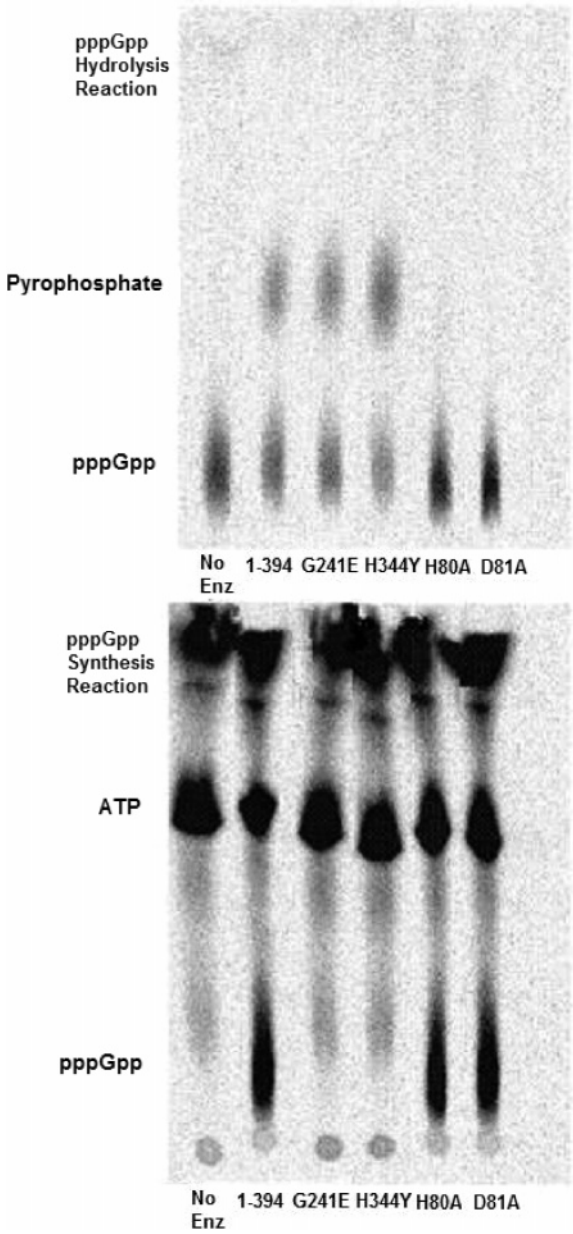

FIGURE 2: Synthesis and hydrolysis capabilities of 1−394, G241E, H344Y, H80A, and D81A. Five microliters of a 30 μL reaction mixture was spotted on a TLC plate, separated, and visualized as described in Materials and Methods. The synthesis reaction that was assayed was *pppA (ATP) + pppG (GTP) ↔ pA (AMP) + pppGpp*. pppGpp* indicates that the radioactive label is on the 3′-βP_i group of the ribose ring of GTP. ATP and GTP concentrations were held constant at 2 mM (1 μCi/μmol of [γ-^{33}P]ATP). The hydrolysis reaction assayed was pppGpp* ↔ pppG (GTP) + pp* (pyrophosphate). The pppGpp concentration was held constant at 0.1 mM. Only radioactive components are visualized. No Enz, the negative control, indicates that no enzyme was added to the reaction mixture.

Also described in our previous study was the fact that addition of uncharged tRNA or the RAC to wild-type Rel_{Mtb} had the opposite effect on hydrolysis activity, increasing $K_{(p)ppGpp}$ 3-fold and decreasing k_{cat} 2-fold. In the study presented here, both uncharged tRNA and the RAC failed to inhibit the activity of the fragments capable of (p)ppGpp hydrolysis (1−181, 1−203, and 1−394).

Evidence of Rel_{Mtb} Multimerization. To determine whether multimerization plays a role in the regulation of Rel_{Mtb}, the protein was studied using analytical gel filtration. Wild-type Rel_{Mtb} formed one distinct peak with an apparent molecular mass of 240 kDa that corresponds to a trimer state (trimer calculated molecular mass of 245 kDa) (Figure 3A). Amino acid fragment 1−394 formed two distinct peaks with apparent molecular masses of 141 and 47 kDa, which correspond to a trimer and monomer state, respectively (trimer calculated molecular mass of 134 kDa and monomer mass of 45 kDa) (Figure 3B). Consistently, more than 75% of the Rel_{Mtb} 1−394 species was purified in the monomer state. Fragment 1−203 formed a major peak (∼95%) with an apparent molecular mass of 28 kDa (monomer calculated molecular mass of 22.7 kDa) which approximates the molecular mass of the monomer state, and a minor peak (∼5%) with an apparent molecular mass of 60 kDa that resembles a multimer state (Figure 3C). The C-terminal end of Rel_{Mtb} (395−738) formed a major peak (∼99%) with an apparent molecular mass of 37 kDa, which corresponds to a monomer state (monomer calculated molecular mass of 37.3 kDa), and a very small peak (∼1%) at 119 kDa corresponding to a trimerized state (trimer calculated molecular mass of 112 kDa) (Figure 3D).

Analysis of Proposed Rel_{Mtb} C-Terminal Multimerization Mutants. Residues C612, D637, and C638 within the C-terminal domain of *E. coli* RelA have been demonstrated to affect oligomerization (*9*). These RelA residues are conserved in Rel_{Mtb} at positions C607, D632, and C633, respectively (Figure 1). The homologous residues in Rel_{Mtb} were mutated, and Rel_{Mtb} variants D632A, D632R, and C633A were expressed in a newly developed *M. smegmatis* expression system and analyzed. Wild-type Rel_{Mtb} and the D632A mutant were expressed in both the *E. coli* and *M. smegmatis* systems. Kinetic parameters of the enzymes were consistent between expression systems. The oligomer state of these mutants was investigated by size exclusion chromatography, and the C-terminal mutants eluted at a size consistent with a trimer.

D632A and D632R had similar catalytic activities, so only D632A was further analyzed. Like wild-type Rel_{Mtb}, D632A and C633A were still activated by uncharged tRNA and the RAC complex during pppGpp synthesis. However, kinetic data revealed important differences between wild-type Rel_{Mtb} and the mutants (D632A and C633A) for the synthesis reaction. First, the mutants showed decreased RAC pppGpp synthesis activity relative to wild-type Rel_{Mtb}: D632A had an approximately 3.5-fold decrease and C633A a 20-fold decrease in RAC synthesis activity compared to wild-type Rel_{Mtb}. Second, although the D632A and C633A mutants exhibited linear pppGpp production during the basal transferase reaction (no RAC) like that of wild-type Rel_{Mtb}, these mutants displayed a significant lag in pppGpp production during the RAC transferase reaction compared to wild-type Rel_{Mtb} (Table 3). The activity lag, defined by the amount of time before a linear rate of activity, was most evident when the enzyme and RAC components (tRNA·ribosome·mRNA complex) were not preincubated together before the reaction was initiated by the addition of substrate (Figure 4 and Table 3, reactions 2, 4, and 7).

To further investigate the effect of enzyme and RAC preincubation on the lag, RAC components and enzyme were preincubated separately or together, for various lengths of time, and at different temperatures before initiation of the reaction (Table 3). To reduce an initial RAC pppGpp

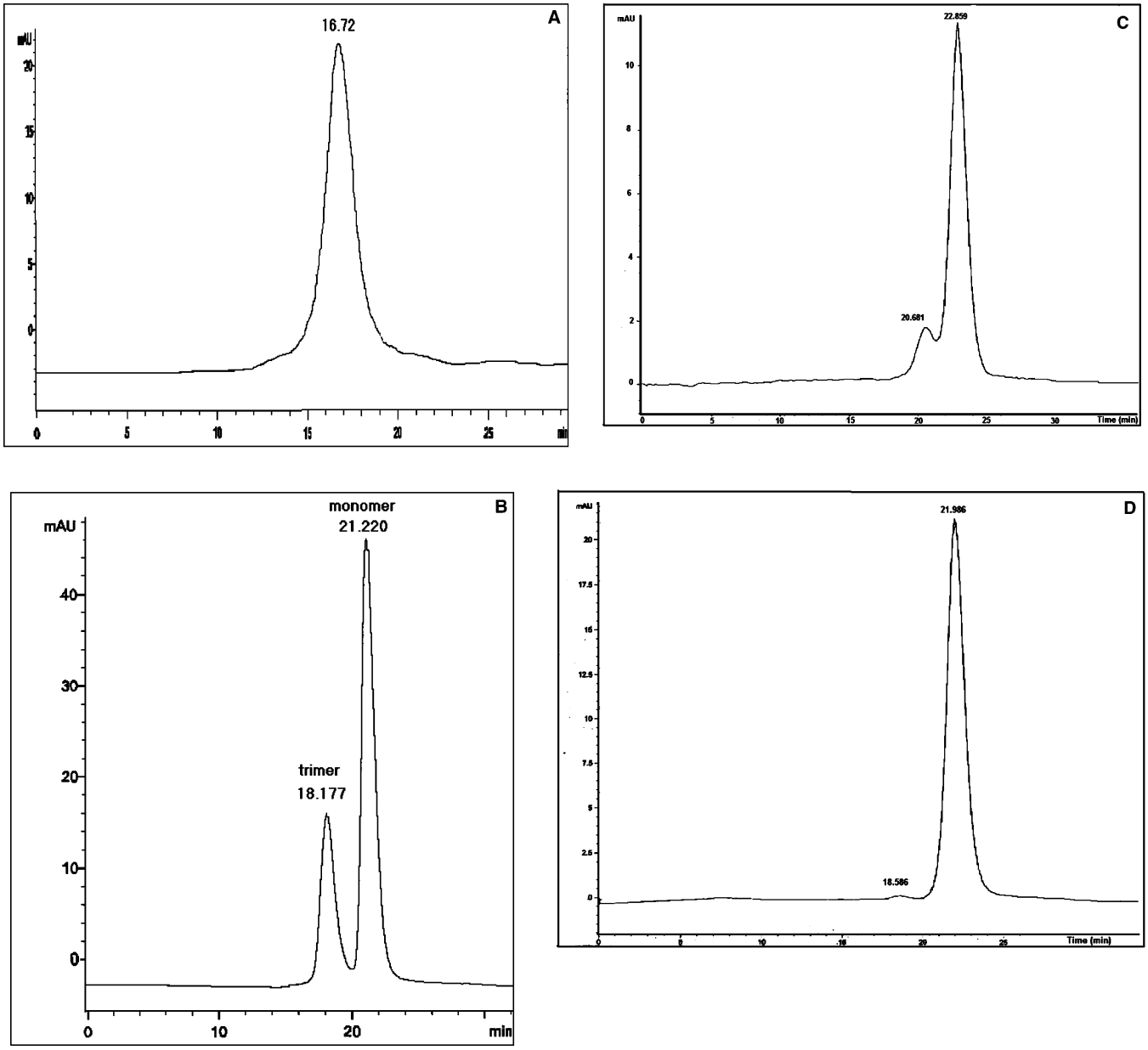

FIGURE 3: Determination of the Rel_{Mtb} multimer state by size exclusion chromatography. HPLC elution monitored at OD_{280} for (A) full-length Rel_{Mtb} (retention time of 16.72 s corresponds to 240 kDa), (B) fragment 1−394 (retention time of 18.1 s corresponds to 141 kDa and a time of 21.2 s corresponds to 47 kDa), (C) fragment 1−203 (retention time of 20.6 s corresponds to 60 kDa and a time of 22.9 s corresponds 28 kDa), and (D) fragment 395−738 (retention time of 18.6 s corresponds to 119 kDa and a time of 22 s corresponds to 37 kDa).

Table 3: Different Degrees of Lag for RAC pppGpp Synthesis[a]

condition	wild type	D632A	C633A
(1) basal synthesis (no RAC)	no lag	no lag	no lag
(2) Enz and RAC preincubated separately on ice for 20 min	14 min	34 min	30 min
(3) Enz and RAC preincubated together on ice for 20 min	9 min	30 min	27 min
(4) Enz and RAC preincubated separately at room temperature for 20 min	9 min	28 min	22 min
(5) Enz and RAC preincubated together at room temperature for 8 min	6 min	22 min	18 min
(6) Enz and RAC preincubated together at room temperature for 20 min	no lag	18 min	16 min
(7) Enz and RAC preincubated separately at 30 °C for 20 min	5 min	24 min	20 min
(8) Enz and RAC preincubated together at 30 °C for 5 min	4 min	14 min	10 min
(9) Enz and RAC preincubated together at 30 °C for 20 min	no lag	no lag	no lag

[a] Monitoring the RAC synthesis reaction of wild-type Rel_{Mtb}, D632A, and C633A every 2 min during a 40 min time course. Times indicate the amount of time of the RAC synthesis lag. Lag is defined by the time delay until linear rates of pppGpp synthesis occur. For the enzyme and RAC preincubated separately, the enzyme is added as the last component to initiate the reaction. For preincubation of enzyme and RAC together, the ATP substrate is added as the last component to initiate the reaction.

synthesis lag, preincubation of enzyme and RAC components was necessary before reaction initiation (Figure 4), and the preincubation effect was temperature- and time-dependent (Table 3). For wild-type Rel_{Mtb}, preincubation of the enzyme

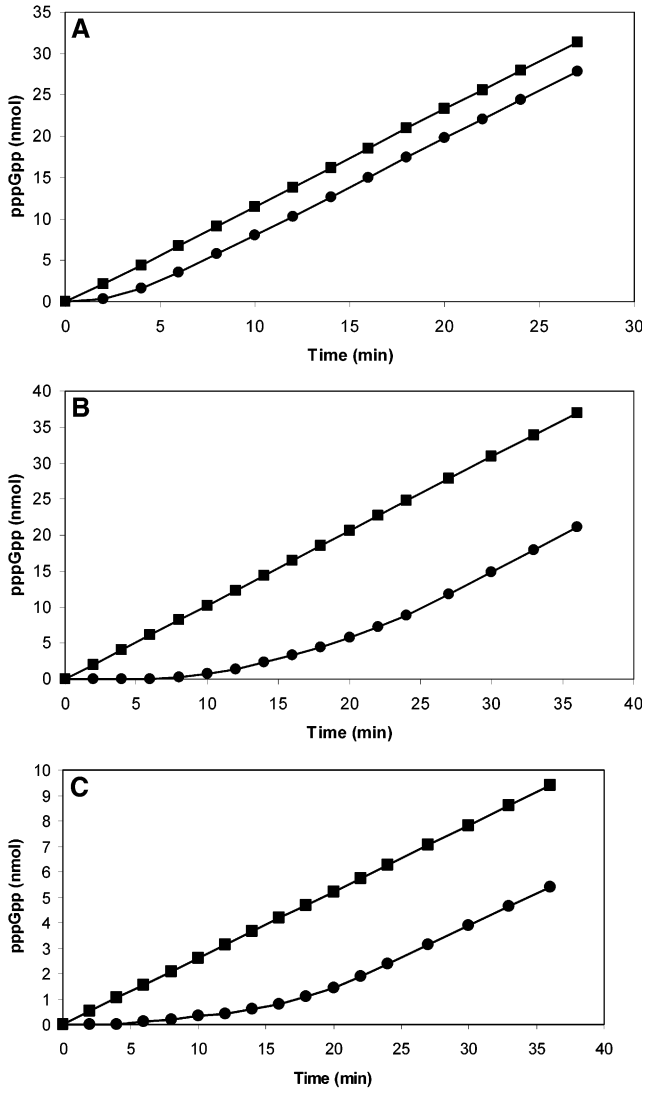

FIGURE 4: RAC pppGpp synthesis reaction monitored as a function of time. Reactions (90 μL) were performed at 30 °C and pH 8.0. ATP and GTP concentrations were held constant at 2 mM. (A) Wild-type Rel_{Mtb}: enzyme and RAC preincubated separately (●) and enzyme and RAC preincubated together (■). (B) D632A mutant enzyme: enzyme and RAC preincubated separately (●) and enzyme and RAC preincubated together (■). (C) C633A mutant enzyme: enzyme and RAC preincubated separately (●) and enzyme and RAC preincubated together (■). For the separate preincubation, the enzyme and RAC were incubated separately at 30 °C for 20 min and then enzyme was added as the last component of the reaction mixture. For preincubation of the enzyme and RAC together, the ATP substrate was added as the last component after enzyme preincubation with RAC components at 30 °C for 20 min.

with RAC components for 20 min at 30 °C or room temperature prior to the reaction prevented a lag in RAC synthesis while preincubation on ice did not (Table 3, reactions 3, 6, and 9). In contrast, for the C-terminal mutant enzymes, only a preincubation with RAC components for 20 min at 30 °C prevented a lag in RAC synthesis (Table 3, reactions 3, 6, and 9). There appeared to be a minimal time requirement for preincubation, as a 5 min preincubation of the enzymes with RAC components at 30 °C decreased the lag, but did not completely alleviate it like the 20 min preincubation (Table 3, reaction 8 vs reaction 9). Despite an initial synthesis lag, reaction rates eventually became linear and equal, regardless of whether RAC components and enzyme were preincubated separately or together (Figure 4A−C).

Stability of Rel_{Mtb} Multimers. Since Rel_{Mtb} fragment 1−394 formed both monomers and trimers, we tested whether an equilibrium existed between the two states. In all purifications of Rel_{Mtb} fragment 1−394, the monomer state would range from 75 to 95% of the total level of species in solution. We therefore tested a 0.6 mg/mL fragment 1−394 solution with 90% monomer and 10% of species in the trimer state as well as a similarly concentrated solution with 75% monomer and 25% trimer to see if there was interconversion between the species. After incubation of these solutions at 30 °C for 100 min, both solutions attained an equilibrium with approximately 75% of the species in the monomer state and 25% of the species in the trimerized state (9 mol of monomer for every 1 mol of trimer). The fragment 1−394 trimer and monomer were each isolated by size exclusion chromatography and run on denaturing SDS−PAGE, and both formed single bands corresponding to a 44 kDa fragment, the size of monomer fragment 1−394.

We next tested whether disulfide bonds were responsible for multimerization. Wild-type Rel_{Mtb} and Rel_{Mtb} fragment 1−394 were incubated with 3 mM DTT for 60 min on ice followed by size exclusion chromatography. The reducing agent did not disrupt the stability of the wild type or the Rel_{Mtb} fragment 1−394 multimer.

Studies similar to those with fragment protein 1−394 were conducted with the fragment proteins 1−203 and 395−738, but no conditions were found to alter the existing monomer-to-multimer ratio.

Fragment 1−394 Monomer and Trimer Equilibrium Studies. After determining that a 0.6 mg/mL fragment 1−394 solution will form an equilibrium consisting of approximately 25% of the species forming trimers and the remaining 75% of the species forming monomers, we next tested elements which might alter this equilibrium. Starting with a fragment 1−394 solution consisting of 13% of the species in the trimer state and 87% of the species forming a monomer state (Figure 5A), we tested whether nucleotide binding would alter the monomer and trimer ratios during incubation at 30 °C over a 45 min time course. Incubation of the fragment 1−394 solution without nucleotides caused an increase in the trimer percentage and resulted in 21% of the species interacting to form trimers and 79% remaining monomers (Figure 5B), thus approaching the equilibrium of 25% trimers and 75% monomers. However, incubation of the fragment 1−394 solution with 2 mM ATP and 2 mM GTP caused a decrease in the original trimer percentage and resulted in only 7% of the species interacting to form trimers and 93% of the species as monomers (Figure 5C). Likewise, the hydrolysis substrate, pppGpp, decreased the trimer percentage in solution, resulting in 6% trimer species and 94% monomer species (Figure 5D).

After isolating the fragment 1−394 trimer by size exclusion chromatography, we monitored its multimerization state during the course of a pppGpp synthesis reaction (Figure 6). When we began with a solution composed of 86% of the species interacting to form trimers and 14% percent of the species in a monomer form (68% moles trimer and 32% moles monomer), 100 min after reaction initiation the solution was composed of 21% of the species in the trimer form and 79% of the species in the monomer from (8% moles

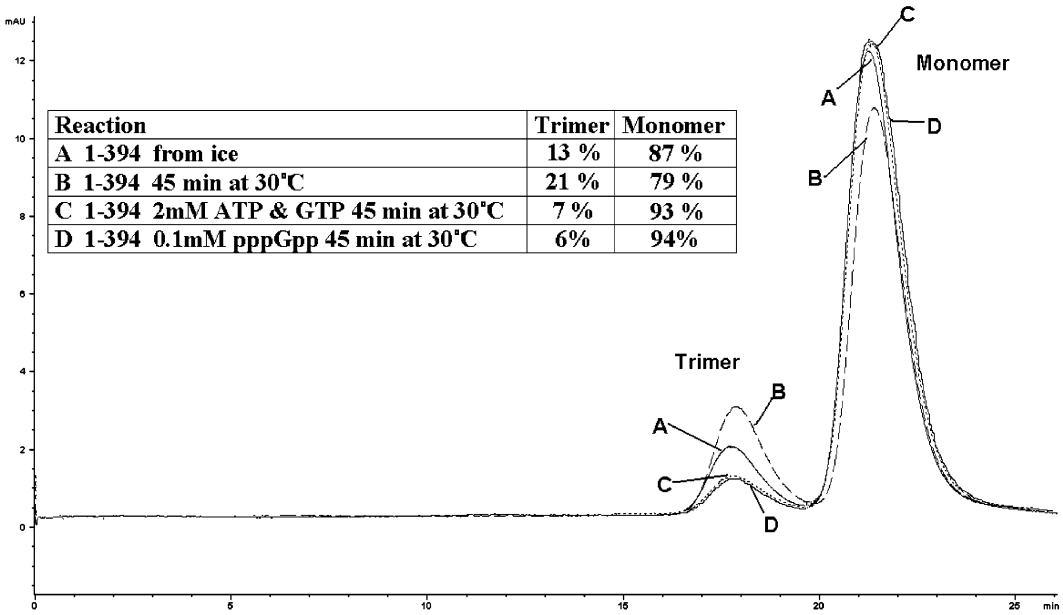

Reaction	Trimer	Monomer
A 1-394 from ice	13 %	87 %
B 1-394 45 min at 30°C	21 %	79 %
C 1-394 2mM ATP & GTP 45 min at 30°C	7 %	93 %
D 1-394 0.1mM pppGpp 45 min at 30°C	6%	94%

FIGURE 5: Monitoring the fragment 1−394 trimer and monomer ratio by size exclusion chromotography. Sixty-five micrograms of fragment 1−394, with 13% of species in the trimer state and 87% of species in the monomer state (time 0 with no 30 °C incubation), was incubated in a 30 μL solution [50 mM HEPES (pH 8.2) and 1 mM DTT] at 30 °C for 45 min with and without nucleotides.

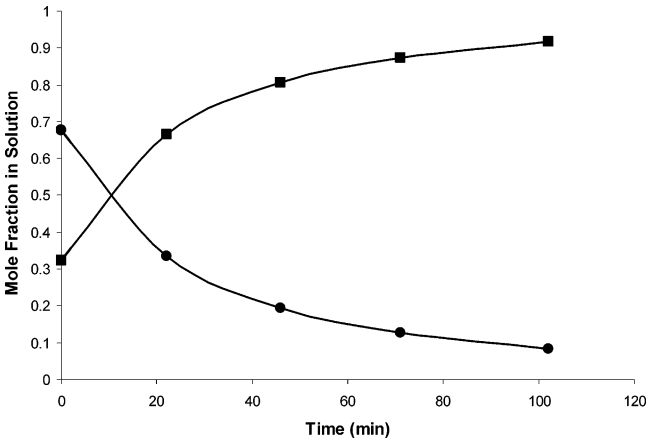

FIGURE 6: Monitoring fragment 1−394 trimer dissociation and corresponding monomer formation during the pppGpp synthesis reaction by size exclusion chromatography. Six hundred microliters of fragment 1−394 trimer synthesis reaction mixture contained 1.5 mM ATP and GTP, 3 mM Mg^{2+}, and 55 μg of fragment 1−394 trimer; 100 μL of the reaction mixture was injected onto a sizing column over a 100 min time course and monitored at OD_{280}. The original solution was composed of 86% trimer species and 14% monomer species, which in mole fraction is 0.68 trimer and 0.32 monomer (trimer, 134 kDa; and monomer, 45 kDa). Trimer dissociation (●), and corresponding monomer formation (■), are represented in terms of mole fraction in solution.

trimer and 92% moles monomer). Since the dissociation of each trimer produces three monomers, we have represented trimer dissociation and monomer formation as the mole fraction of species in solution (Figure 6).

Activity of the Isolated Fragment 1−394 Monomer and Trimer. After separating the fragment 1−394 monomer from the trimer by size exclusion chromatography, we separately assayed the isolated monomer and isolated trimer for pppGpp synthesis and hydrolysis activity and compared their relative activities. Synthesis and hydrolysis reaction mixtures for each species contained equal concentrations of total enzyme (0.02 mg/mL): 374 nM fragment 1−394 monomer (44.5 kDa) for the monomer reaction and 124 nM fragment 1−394 trimer (133.7 kDa) for the trimer reaction. The pppGpp synthesis and hydrolysis activities of the isolated fragment 1−394 monomers were at least 3 times greater than that of the isolated trimers at the same enzyme concentration (Table 4 reaction 1 vs reaction 2, and Table 5, reaction 1 vs reaction 2). Therefore, 1 mole of monomer has at least the same activity as 1 mole of trimer (Table 4, reaction 1 vs reaction 2, and Table 5, reaction 1 vs reaction 2). Because the trimer dissociates over the course of a reaction and both the trimer and monomer lose activity over the course of a reaction, we

Table 4: Kinetic Constants for the Rel_{Mtb} Fragment 1−394 Ribosome-Independent Synthesis Reaction[a]

synthesis reaction	k_{cat} (s^{-1})	normalized activity at the same enzyme concentration
(1) fragment 1−394 Rel_{Mtb} monomer (45 kDa)	0.66 ± 0.04	3
(2) fragment 1−394 Rel_{Mtb} trimer (135 kDa)	≤0.66 ± 0.04	≤1

[a] Comparison of synthesis activity of the isolated fragment 1−394 monomer and isolated fragment 1−394 trimer. Reaction mixtures contained equal concentrations of each species. At the same concentration, there are 3 times more moles of fragment 1−394 trimer than fragment 1−394 monomer.

Table 5: Kinetic Constants for the Rel_{Mtb} Fragment 1−394 Ribosome-Independent Hydrolysis Reaction[a]

hydrolysis reaction	mol of PP_i s^{-1} (mol of enzyme)$^{-1}$	normalized activity at the same enzyme concentration
(1) fragment 1−394 Rel_{Mtb} monomer (45 kDa)	0.027	3
(2) fragment 1−394 Rel_{Mtb} trimer (135 kDa)	≤0.027	≤1

[a] Comparison of hydrolysis activity of the isolated fragment 1−394 monomer and the isolated fragment 1−394 trimer. Reaction mixtures contained equal concentrations of each species. At the same concentration, there are 3 times more moles of fragment 1−394 trimer than fragment 1−394 monomer.

only determined with certainty that 1 mol of trimer has the same activity as or less activity than 1 mol of monomer (Tables 4 and 5).

DISCUSSION

In the Gram-negative bacterium *E. coli*, two proteins are responsible for the synthesis and hydrolysis of (p)ppGpp: the RelA protein synthesizes (p)ppGpp in response to amino acid starvation, and the SpoT protein hydrolyzes (p)ppGpp. Under certain conditions, SpoT is also capable of synthesizing (p)ppGpp, but RelA is not capable of hydrolyzing (p)ppGpp. Results of deletion analysis (*8*) of the *spoT* gene in *E. coli* identified mutants that contain either one activity or the other: residues 1−203 contain the domain for (p)ppGpp degradation, while residues 85−375 contain the domain for (p)ppGpp synthesis. The SpoT protein is related to the Gram-positive, dual-function Rel class of proteins, and it is hypothesized that the *spoT* and *relA* genes evolved from the gene duplication of an ancestral *rel*-like gene (*12*). Thus, it is likely that Rel_{Mtb} from the Gram-positive organism *M. tuberculosis*, which carries out both synthesis and hydrolysis of (p)ppGpp, will have separate catalytic domains like the SpoT protein of *E. coli* (*8*). Mechold and colleagues demonstrated separate catalytic domains in a Rel homologue from *Streptomyces equisimilis*, Rel_{seq}: residues 1−224 contain the domain for (p)ppGpp degradation, and residues 79−385 contain the domain for (p)ppGpp synthesis (*13*). The recent crystallization of the catalytic half of Rel_{seq} (residues 1−385) places the synthetase and hydrolase active sites more than 30 Å apart (*11*). Consistent with these studies, our biochemical study also indicates that Rel_{Mtb} catalytic activities are located in distinct domains in the N-terminus and the regulatory domains are present in the C-terminus.

Our current results support the conclusion from our previous study based on kinetic evidence that the transferase and hydrolysis reactions of Rel_{Mtb} are catalyzed at distinct active sites (*7*). Rel_{Mtb} fragment 1−181 is only capable of (p)ppGpp hydrolysis, and protein fragment 87−394 is only capable of (p)ppGpp synthesis (Figure 1). Furthermore, a fragment 395−738 is devoid of all activity. The pppGpp hydrolysis activity of fragment protein 1−181 is significantly decreased compared to those of fragment 1−394, fragment 1−203, and wild-type Rel_{Mtb} (Table 2), possibly because of an unidentified domain disruption or decreased protein stability. Otherwise, Rel_{Mtb} hydrolysis-only fragment 1−203 and dual-function Rel_{Mtb} fragment 1−394 have pppGpp hydrolysis activity similar to that of wild-type Rel_{Mtb}, which is in contrast to the 150-fold reduction in hydrolysis activity of similar C-terminal deletions in the Rel_{seq} system (*13*). Deletion of the C-terminal end of full-length Rel_{Mtb} (residues 1−394 or 87−394) does not greatly affect the basal level of pppGpp synthesis either (Table 1), which is in contrast to the Rel_{seq} system where a weak (p)ppGpp synthesis activity in full-length Rel_{seq} is activated 12-fold by a C-terminal deletion (*13*). Mechold and colleagues suggest that a C-terminal deletion in the Rel_{seq} system is analogous to the effect by the RAC in synthesis activation and hydrolysis reduction for wild-type Rel_{Mtb} (*13*). These observations suggest that in both the Rel_{seq} and Rel_{Mtb} systems the C-terminus is necessary to respond to amino acid deprivation, but the two species have evolved different strategies for utilizing the C-terminus based on their environmental niches.

While the Rel_{Mtb} (p)ppGpp synthesis and hydrolysis activities can be isolated on different fragment proteins, the protein fragments share an overlapping region of amino acids 87−181 (Figure 1). In *E. coli* SpoT, an overlapping region is necessary for (p)ppGpp synthesis and hydrolysis activities (*8*) and the Rel_{seq} crystal structure reveals that residues in this overlapping region are important for nucleotide binding (*11*). Much of this overlap occurs in a predicted region known as the HD domain, named for the conserved histidine and aspartate doublet in this region (Figure 1A) (*10*). On the basis of the catalytic properties of enzymes with this domain, the conserved H and D residues are predicted to be essential for coordinating divalent cations needed for activity (*10*). Rel_{seq} crystal structure analysis locates a manganese ion coordinated by a group of residues that includes the HD doublet (*11*). An HD domain in Rel_{Mtb} was identified using the PSI-BLAST program with amino acids 49−159 from the SMART database (*14*, *15*). Deletion of the terminal amino acids of this domain may remove necessary active site residues for (p)ppGpp hydrolysis and thus may explain the inactivity of amino acid fragment 1−156 (Figure 1F). Likewise, while much of the HD domain is present in (p)ppGpp synthesis-only fragment 87−394, the conserved histidine and aspartate doublet as well as the N-terminal portion of this domain are absent, suggesting the necessity of these residues for (p)ppGpp hydrolysis (Figure 1G). Both the H80 and D81 residues were mutated in Rel_{Mtb} to alanines, and each residue was found to be essential for pppGpp hydrolysis, but not required for pppGpp synthesis (Figure 2). Although Rel_{Mtb} pppGpp synthesis is supported by manganese, the H80 and D81 residues do not appear to have a role in manganese coordination for the synthesis reaction. *E. coli* RelA contains substitutions of the predicted histidine and aspartate doublet, which may account for the fact that RelA has only (p)ppGpp synthesis activity (*8*, *10*).

Gropp and colleagues found that the *E. coli* RelA G251E mutation impaired both ATP and GTP binding and caused a complete loss of RelA (p)ppGpp synthesis ability in culture, which agreed with the observation of the analogous spontaneous *Bacillus subtilis* mutant that lacked a stringent response and (p)ppGpp synthesis (*9*, *16*). Gropp further found that a RelA H354Y mutation impaired ATP binding and caused a partial loss of synthetic activity (*9*). RelA G251 and H354 are conserved in wild-type Rel_{Mtb} and correspond to Rel_{Mtb} G241 and H344, respectively (Figure 1A). These two residues are also conserved in Rel_{seq}, and crystal analysis indicates their proximity to binding pockets for the synthesis substrates (*11*). Both the Rel_{Mtb} G241E and H344Y purified mutants failed to synthesize pppGpp, while their pppGpp hydrolytic capability was not impaired (Figure 2). These essential residues are present in the protein fragments capable of pppGpp synthesis (1−394, 1−450, and 87−394) but absent in the fragments incapable of pppGpp synthesis (1−203 and 1−181) (Figure 1D,E).

Wild-type Rel_{Mtb} synthesis activity is activated 2-fold from basal levels by uncharged tRNA alone and 80-fold by a complex of uncharged tRNA, ribosomes, and cognate mRNA (RAC) (*7*). The inability of Rel_{Mtb} synthesis fragments 1−394 and 1−450 to be activated above basal levels by the RAC (Table 1) indicates that the 288 C-terminal amino acids contain an area of Rel_{Mtb} regulation (Figure 1). This agrees with work by Metzger and Schreiber (*17*, *18*), who found

that the N-terminal domain (residues 1−455) of RelA contains the catalytic domain and the C-terminal domain (residues 455−744) of RelA is involved in regulating activity. Yang has also reported that the RelA amino acid region from residue 455 to the C-terminus represents the ribosome binding domain of the protein (*19*). This ribosomal binding area identified by Yang corresponds to the Rel_{Mtb} region from residue 449 to the C-terminus (Figure 1A).

Using bacterial two-hybrid analysis, *E. coli* RelA was found to form oligomers, mediated by its C-terminal domain (*9*). Amino acid residues 455−538 and 550−682 in RelA, corresponding to residues 449−535 and 547−676 in Rel_{Mtb}, respectively (Figure 1A), have been demonstrated to take part in dimerization (*19*). Our results from gel filtration assays indicate that wild-type Rel_{Mtb} is capable of forming trimers (Figure 3A). Rel_{Mtb} fragment 1−394 forms both monomers and trimers (Figure 3B), but monomers are predominantly observed. This suggests (i) the C-terminal region of the full-length protein may have interactions responsible for multimerization, (ii) the region around amino acid 394 may be important for multimerization, and/or (iii) the N-terminus contains amino acids sufficient for multimerization. Gropp demonstrated interactions between the C-termini of RelA and weak interactions of full-length RelA with the N-terminus of RelA (*9*). We observed more than 99% of Rel_{Mtb} fragment 395−738 is in the monomer state, suggesting residues in the terminal 344 amino acids are not sufficient for stable multimerization (Figure 3D). To determine if N-terminal interactions play a role in multimerization, we tested whether fragment protein 1−203 could form multimers. We observed a predominantly monomer state, with a potential multimer state with fragment 1−203, indicating the N-terminus alone is not sufficient for stable multimerization (Figure 3C).

RelA mutation analysis suggests that amino acids C612, D637, and C638, which are part of a highly conserved 27-amino acid sequence in RelA homologues, are important for RelA oligomerization (*9*). These three amino acids are conserved at positions C607, D632, and C633 in Rel_{Mtb} (Figure 1A), and overall Rel_{Mtb} is 67% homologous to the conserved 27-amino acid sequence of RelA. The oligomerization state of the D632A and C633A mutants in Rel_{Mtb} was assessed by size exclusion chromatography, but mostly large aggregations eluted in the void volume. This was also a problem for wild-type Rel_{Mtb}, so we believe the full-length proteins are highly unstable and precipitate on the sizing column. On several occasions, we observed an elution profile that was consistent with trimer formation, and we suggest that residues D632 and C633 are neither sufficient for Rel_{Mtb} multimerization nor solely responsible for preventing multimerization. Furthermore, since high concentrations of DTT did not disrupt multimer formation, we also suggest that Rel_{Mtb} multimerization is not due to disulfide bonds from the C607 or C633 residues, but rather from strong noncovalent interactions.

Biochemical analysis of the purified D632A and C633A Rel_{Mtb} mutants revealed a notable lag in their pppGpp synthesis activity compared to wild-type Rel_{Mtb} during reactions with RAC components (Table 3 and Figure 4A−C). This delayed synthesis activity was not present during basal activity (absence of the RAC) (Table 3). The delay in the (p)ppGpp synthesis rate was relieved after the enzyme was preincubated with RAC components for 20 min at 30 °C (Figure 4A−C), indicating that the aspartate and cysteine residues are important for association of Rel_{Mtb} with the RAC. Whether the D632A or C633A mutation causes a direct association problem between the protein and RAC components or a possible disruption in the multimerization interface of the protein and subsequent altered association with RAC components has yet to be determined.

Kinetic analysis of the isolated fragment 1−394 monomer indicates pppGpp synthetic and hydrolytic activities similar to those of wild-type Rel_{Mtb} (Table 1, reaction 1 vs reaction, and Table 2, reaction 1 vs reaction 2). However, the isolated fragment 1−394 trimer displayed an unusual increase in activity over time. The increased rate of activity over time for the isolated fragment 1−394 trimer was due to its dissociation into more active monomer components (Figure 6). By comparing the activity of the isolated trimer with that of the isolated monomer and factoring in the dissociation of the trimer over time, we calculated 1 mol of fragment 1−394 Rel_{Mtb} trimer has activity approximately equal to 1 mol of fragment 1−394 Rel_{Mtb} monomer for both pppGpp synthesis and hydrolysis (Tables 4 and 5). It is possible that the fragment 1−394 Rel_{Mtb} trimer may not be active and all activity that is observed is actually due to dissociated monomers. Although this is a possibility, it is more likely that the trimer state is active since the wild-type Rel_{Mtb} is assayed in a purified trimer state, and we have always observed constant basal activity rates over time rather than an increase in rate due to dissociation of the trimer into monomer components. Wild-type Rel_{Mtb} could very rapidly dissociate into monomer components during the basal reaction or RAC reaction, thus requiring more precise techniques for monitoring of this activity.

The isolated fragment 1−394 trimer dissociates during the course of pppGpp synthesis (Figure 6), but maintains an equilibrium of trimer and monomer species when not incubated with substrate, suggesting that nucleotide binding may affect the monomer and trimer distribution. Substrate binding causes a dissociation of the fragment 1−394 trimer into monomer components (Figure 5). In Rel_{seq} fragment 1−385, synthesis and hydrolysis substrates seem to lock each individual monomer within the crystallized unit into a conformation suitable for either (p)ppGpp synthesis or hydrolysis (*11*). Because full-length Rel_{Mtb} simultaneously catalyzes its opposing reactions at maximal rates during basal activity (*7*), we suggest the same locked state does not exist for Rel_{Mtb}. However, rather than affecting the opposing activity on the same monomer, nucleotide binding to one of the monomers within the fragment 1−394 Rel_{Mtb} trimer could prevent the other two monomers from having activity. The fragment 1−394 Rel_{Mtb} shift to the monomer state upon substrate binding may prevent inactive monomer components from becoming tied up in a multimer state. While substrate binding causes a shift toward the monomer state for fragment 1−394, we do not yet know the effects on the full-length protein. Nucleotide binding may represent a means of controlling the trimer and monomer ratio and subsequent activity of the protein.

Wild-type Rel_{Mtb} was found to exclusively form trimers in vitro (Figure 3A), so we predict that Rel_{Mtb} maintains a trimer state during normal growth conditions in vivo. A proper multimerization configuration may be necessary for

Rel_{Mtb} to bind uncharged tRNA, as is the case for GCN2 and class II tRNA synthetases (*20*, *21*). On the basis of kinetic evidence that the trimer state may contain two catalytically inactive monomers, we suggest that trimerized Rel_{Mtb} may be an environmentally responsive state while the monomer state is the highly active state. Crystal structure analysis, NMR analysis, and investigation of tRNA and ribosome binding with Rel_{Mtb} will help elucidate this mechanism further.

ACKNOWLEDGMENT

We thank Drs. Norman Schechter and Michael Plotnick for their helpful discussions.

REFERENCES

1. World Health Organization (1998) *The WHO/IUATLD Global Project on Anti-tuberculosis*, Drug Resistance Surveilance 1994−1997, World Health Organization, Geneva, Switzerland.
2. Raviglione, M. C. (2002) *4th World Congress on Tuberculosis Program/WHO*, Vol. 2, World Health Organization, Geneva, Switzerland.
3. Hu, Y. M., Butcher, P. D., Sole, K., Mitchison, D. A., and Coates, A. R. (1998) Protein synthesis is shutdown in dormant *Mycobacterium tuberculosis* and is reversed by oxygen or heat shock, *FEMS Microbiol. Lett. 158*, 139−145.
4. Avarbock, D., Salem, J., Li, L. S., Wang, Z. M., and Rubin, H. (1999) Cloning and characterization of a bifunctional RelA/SpoT homologue from *Mycobacterium tuberculosis*, *Gene 233*, 261−269.
5. Primm, T. P., Andersen, S. J., Mizrahi, V., Avarbock, D., Rubin, H., and Barry, C. E. (2000) The stringent response of *Mycobacterium tuberculosis* is required for long-term survival, *J. Bacteriol. 182*, 4889−4898.
6. Dahl, J. L., Kraus, C. N., Boshoff, H. I., Doan, B., Foley, K., Avarbock, D., Kaplan, G., Mizrahi, V., Rubin, H., and Barry, C. E. (2003) The role of RelMtb-mediated adaptation to stationary phase in long-term persistence of *Mycobacterium tuberculosis* in mice, *Proc. Natl. Acad. Sci. U.S.A. 100*, 10026−10031.
7. Avarbock, D., Avarbock, A., and Rubin, H. (2000) Differential regulation of opposing RelMtb activities by the aminoacylation state of a tRNA·ribosome·mRNA·RelMtb complex, *Biochemistry 39*, 11640−11648.
8. Gentry, D. R., and Cashel, M. (1996) Mutational analysis of the *Escherichia coli* spoT gene identifies distinct but overlapping regions involved in ppGpp synthesis and degradation, *Mol. Microbiol. 19*, 1373−1384.
9. Gropp, M., Strausz, Y., Gross, M., and Glaser, G. (2001) Regulation of *Escherichia coli* RelA requires oligomerization of the C-terminal domain, *J. Bacteriol. 183*, 570−579.
10. Aravind, L., and Koonin, E. V. (1998) The HD domain defines a new superfamily of metal-dependent phosphohydrolases, *Trends Biochem. Sci. 23*, 469−472.
11. Hogg, T., Mechold, U., Malke, H., Cashel, M., and Hilgenfeld, R. (2004) Conformational antagonism between opposing active sites in a bifunctional RelA/SpoT homolog modulates (p)ppGpp metabolism during the stringent response, *Cell 117*, 57−68.
12. Mittenhuber, G. (2001) Comparative genomics and evolution of genes encoding bacterial (p)ppGpp synthetases/hydrolases (the Rel, RelA and SpoT proteins), *J. Mol. Microbiol. Biotechnol. 3*, 585−600.
13. Mechold, U., Murphy, H., Brown, L., and Cashel, M. (2002) Intramolecular regulation of the opposing (p)ppGpp catalytic activities of Rel(Seq), the Rel/Spo enzyme from *Streptococcus equisimilis*, *J. Bacteriol. 184*, 2878−2888.
14. Schultz, J., Milpetz, F., Bork, P., and Ponting, C. P. (1998) SMART, a simple modular architecture research tool: Identification of signaling domains, *Proc. Natl. Acad. Sci. U.S.A. 95*, 5857−5864.
15. Letunic, I., Goodstadt, L., Dickens, N. J., Doerks, T., Schultz, J., Mott, R., Ciccarelli, F., Copley, R. R., Ponting, C. P., and Bork, P. (2002) Recent improvements to the SMART domain-based sequence annotation resource, *Nucleic Acids Res. 30*, 242−244.
16. Wendrich, T. M., and Marahiel, M. A. (1997) Cloning and characterization of a relA/spoT homologue from *Bacillus subtilis*, *Mol. Microbiol. 26*, 65−79.
17. Metzger, S., Schreiber, G., Aizenman, E., Cashel, M., and Glaser, G. (1989) Characterization of the relA1 mutation and a comparison of relA1 with new relA null alleles in *Escherichia coli*, *J. Biol. Chem. 264*, 21146−21152.
18. Schreiber, G., Metzger, S., Aizenman, E., Roza, S., Cashel, M., and Glaser, G. (1991) Overexpression of the relA gene in *Escherichia coli*, *J. Biol. Chem. 266*, 3760−3767.
19. Yang, X., and Ishiguro, E. E. (2001) Dimerization of the RelA protein of *Escherichia coli*, *Biochem. Cell Biol. 79*, 729−736.
20. Qiu, H., Dong, J., Hu, C., Francklyn, C. S., and Hinnebusch, A. G. (2001) The tRNA binding moiety in GCN2 contains a dimerization domain that interacts with the kinase domain and is required for tRNA binding and kinase activation, *EMBO J. 20*, 1425−1438.
21. Eriani, G., Cavarelli, J., Martin, F., Dirheimer, G., Moras, D., and Gangloff, J. (1993) Role of dimerization in yeast aspartyl-tRNA synthetase and importance of the class II invariant proline, *Proc. Natl. Acad. Sci. U.S.A. 90*, 10816−10820.

BI0505316